Heat Mass Transfer (2005) 41: 625–631
DOI 10.1007/s00231-004-0579-4

ORIGINAL

Anna Angela Barba

Thermal treatments of foods: a predictive general-purpose code for heat and mass transfer

Received: 11 March 2004 / Accepted: 11 November 2004 / Published online: 4 March 2005

Abstract Thermal treatments of foods required accurate processing protocols. In this context, mathematical modeling of heat and mass transfer can play an important role in the control and definition of the process parameters as well as to design processing systems. In this work a code able to simulate heat and mass transfer phenomena within solid bodies has been developed. The code has been written with the ability of describing different geometries and it can account for any kind of different initial/boundary conditions. Transport phenomena within multi-layer bodies can be described, and time/position dependent material parameters can be implemented. Finally, the code has been validated by comparison with a problem for which the analytical solution is known, and by comparison with a differential scanning calorimetry signal that described the heating treatment of a raw potato (*Solanum tuberosum*).

1 Introduction

Thermal unit operations, such as sterilization, drying and cooking, but also freeze-drying and thawing, are often adopted to stabilize, preserve, make suitable for consumption or obtain longer shelf-life of food products. In order to obtain processed products that keep more of their original characteristics (flavors and nutritional values, color and texture, rehydratation content) thermal treatments required accurate processing protocols [1]. In this context, mathematical modeling of heat and mass transfer in foods during thermal treatment can play an important role in the control and definition of the process parameters as well as to design processing systems.

The heat and mass transfer phenomena within solid bodies have been investigated extensively. The modeling issues have been established from a long time (e.g. Ref. [2]), and the analytical solutions have been found for a large number of problems [3, 4]. However, as it has already been pointed out in recent works, in both industrial and R&D practical problems, for which analytical solutions are not known, are very common. These problems are simple in principle, but are complicated by some particular features. In particular, material characteristics as well as generation terms can vary with both independent (time, position) and dependent (temperature, concentrations) variables, and heat and mass transfer phenomena can interact to each other (the balance equations result to be coupled). In these conditions, analytical solutions are extremely rare.

In a preliminary work [5] it was suggested the basic structure of a code able to simulate transient one-dimensional heat transfer phenomena, for different geometries, and the code was validated by comparison with a number of analytical solutions. In subsequent works, coupling the heat balance and a mass balance accounting for mass generation/consumption increased the capability of the code. This improved code version has been applied in studies of polymer crystallization during the cooling in a DSC apparatus [6], and in studies of microwave heating of different dielectric materials in microwave single-mode cavity [7].

Aim of this work is to further improve the code, adding the ability to simulate mass diffusion phenomena and heat and mass transport phenomena in multi-layer systems. As usual, firstly the code will be validated by comparison with a problem for which the analytical solution is known, and afterwards a real situation (heating of foodstuff in DSC) will be simulated to test the ability of the code to reproduce real processes.

A. A. Barba
Department of Chemical and Food Engineering,
University of Salerno, via Ponte don Melillo,
84084 Fisciano (Salerno), Italy
E-mail: aabarba@unisa.it
Tel.: +39-089-964026
Fax: +39-089-964057

2 Modeling

The code written to solve generalized energy balance has already been described in a previous paper [5]. An improved version also accounting for mass generation/consumption or phase change has been adopted to describe polymer crystallization by cooling of slabs [6] and heating of cylinder workloads by microwave in a single-mode applicator [7]. In the current work, the mass balance has been further improved to take in account for diffusion or pseudo-diffusion phenomena. Both the balances (energy and mass) assume the same structure (Eq. 1), and they naturally result to be coupled via material parameters and generation terms, as well as via boundary conditions, which are detailed in the following.

$$\frac{\partial \Gamma_i(t,\xi)}{\partial t} = A_i(t,\xi)\left(\frac{f}{\xi}\frac{\partial \Gamma_i(t,\xi)}{\partial \xi} + \frac{\partial^2 \Gamma_i(t,\xi)}{\partial \xi^2}\right) + B_i(t,\xi) \quad (1)$$

In Eq. 1, t is the time variable and ξ is the space variable while $\Gamma_i(t, \xi)$ is the dependent variable (temperature or mass concentration). Material characterizing parameters and generation terms are accounted for in the terms A_i and B_i, respectively. The values assumed by all the terms reported in Eq. 1 are summarized in Table 1. Flag f can be zero, one or two, describing the heat transfer problem in a semi-infinite flat slab ($\xi \equiv z$ = axial direction), in a semi-infinite cylinder ($\xi \equiv r$ = radial direction) or in a sphere ($\xi \equiv r$ = radial direction), respectively. The new version of the code is able to solve simultaneously two PDEs with the structure given by Eq. 1 ($i = 1, 2$), that could describe heat and mass balances, as well as isothermal coupled mass balances.

In principle the diffusion term in Eq. 1, with reference to rectangular coordinates, should be written as

$$\frac{\partial}{\partial \xi}\left(A\frac{\partial \Gamma}{\partial \xi}\right) = \frac{\partial A}{\partial \xi}\frac{\partial \Gamma}{\partial \xi} + A\frac{\partial^2 \Gamma}{\partial \xi^2} = \frac{\partial A}{\partial \Gamma}\frac{\partial \Gamma}{\partial \xi}\frac{\partial \Gamma}{\partial \xi} + A\frac{\partial^2 \Gamma}{\partial \xi^2}$$

However, the philosophy of numerical solution of PDEs is to keep the derivatives as little as possible to minimize the errors due to the replacement of the derivatives themselves by finite differences. Thus, the first term on right-hand side of the above reported equation, being built multiplying three derivative terms, is negligible if compared with the other terms. In conclusion, Eq. 1 is a good starting point for simulation of transient/diffusive phenomena, even if the parameters are not constant.

The model has to be completed by suitable initial and boundary conditions. Standard form of Initial Conditions (I.C.) is given by Eq. 2a ($i = 1, 2$):

Table 1 Meanings of symbols in Eqs. 1 and 2

	i	Γ_i	A_i	B_i	C_i
Heat	1	T	$\alpha_{T,j}$	$\alpha_{\mathrm{T,j}}/k_{\mathrm{T,j}}\ G_{\mathrm{T,j}}$	$k_{T,j}$
Mass	2	C	D_j	$D_j/a_j\ G_{\mathrm{M,j}}$	D_j

$$\text{I.C.} \quad \Gamma_i(t=0,\xi) = \Gamma_i^0(\xi) \quad (2a)$$

where Γ_i^0 (ξ) are the initial distributions of the two dependent variable Γ_1 and Γ_2.

Boundary conditions (B.C.) can be written in a generalized form ($i = 1, 2$):

$$\text{B.C. (A)}, \ \xi = \Xi_A \quad \alpha_{A,i}\frac{\partial \Gamma_i}{\partial \xi} + \beta_{A,i}\Gamma_i + \gamma_{A,i} = 0 \quad (2b)$$

$$\text{B.C. (B)}, \ \xi = \Xi_B \quad \alpha_{B,i}\frac{\partial \Gamma_i}{\partial \xi} + \beta_{B,i}\Gamma_i + \gamma_{B,i} = 0 \quad (2c)$$

In Eq. 2b $\alpha_{A,i}(t)$, $\beta_{A,i}(t)$ and $\gamma_{A,i}(t)$ are parameters useful to reproduce usual forms of boundary conditions for the boundary at $\xi = \Xi_A$. The same task, at $\xi = \Xi_B$, was played by $\alpha_{B,i}(t)$, $\beta_{B,i}(t)$ and $\gamma_{B,i}(t)$ in Eq. 2c. A detailed description of the values that the coefficients assume for different boundary conditions was reported in Barba and Lamberti [5].

The spatial domain comprised between $\xi = \Xi_A$ and $\xi = \Xi_B$ can be subdivided into J different layers, in perfect thermal contact, made by different materials (of course, the value of A_i and B_i have to be built to take in account for the change of the material). In correspondence of the separation surfaces, the code works verifying the "Continuity Conditions", i.e. the dependent variables Γ_i and their fluxes have to be continuous. Mathematically, this means that Eqs. 2d have been implemented in the code.

$$\text{C.C.}, \ \xi = \Xi_j (j = 1, \ldots, J) \quad \begin{cases} \Gamma_i|_{\xi^-} = \Gamma_i|_{\xi^+} \\ C_{i,j-1}\left.\frac{\partial \Gamma_i}{\partial \xi}\right|_{\xi^-} = C_{i,j}\left.\frac{\partial \Gamma_i}{\partial \xi}\right|_{\xi^+} \end{cases} \quad (2d)$$

All the parameters adopted in Eqs. 1 and 2 are summarized in Table 1. The meaning of index i and j are, respectively, the nature of the dependent variable (temperature or concentration) and the number of layers considered. Physical meaning of all the parameters comes from common use (α_{T}, thermal diffusivity $\mathrm{m^2\ s^{-1}}$; k_{T}, thermal conductivity, $\mathrm{J\ s^{-1}\ K^{-1}\ m^{-1}}$; D, pseudo-diffusion coefficient, $\mathrm{m^2\ s^{-1}}$). It is worth noticing that the coupling between the two balances could be obtained by properly setting the generation terms $G_{T,j}$ and $G_{M,j}$ which can be built as functions of the time, the position, the Γ_i and the Γ_i time derivative.

The partial differential equations (Eq. 1), with their initial, boundary and "continuity" conditions (Eq. 1) ($i = 1, 2$), were solved by the finite difference method known as Crank–Nicolson scheme as described by Lapidus and Pinder [8].

3 A preliminary validation: simultaneous diffusion of heat and moisture

Crank [4, Chap. 15] analyzed a problem in which heat and mass were transferred simultaneously, the

non-isothermal uptake of water by a package made by textile fibers and air entrapped in the fibers. An analytical solution, due to Henry [9, 10] is reported and discussed in Crank [4], and here in the following the problem and the solution are briefly summarized. The heat and mass transfer equations are

$$\rho C_P \frac{\partial T}{\partial t} = k_T \frac{\partial^2 T}{\partial x^2} + \rho \Delta H \frac{\partial M}{\partial t} \tag{3a}$$

$$v \frac{\partial C}{\partial t} = vD \frac{\partial^2 C}{\partial x^2} - (1-v)\rho_s \frac{\partial M}{\partial t} \tag{3b}$$

In Eq. 3, T is the fiber temperature, M the amount of the moisture absorbed by unit mass of fiber, C the concentration of water vapor in the air spaces t the time and x is the position along which the transport phenomena take place. The other parameters: ρ is the density of the package (textile fiber + air void), C_P is the specific heat of the package, k_T is the heat conductivity of the package, ΔH is the heat evolved for mass unity in vapor absorption by the fiber, v is the fraction of the package volume occupied by the air (whereas $1-v$ is the fraction occupied by the fiber), ρ_s is the density of the fiber and D is the diffusion coefficient for the moisture in air. The moisture in the fiber can be related to water concentration in air and temperature (C and T) by a linear relationship [4, p. 355]:

$$M = M^0 + \sigma C - \omega T \tag{3c}$$

where M^0 is a reference moisture, σ and ω are empirical coefficients.

If a package, in equilibrium with its surroundings at given values of temperature and concentration of vapor in air (T_0 and C_0), is exposed to sudden changes in external conditions, i.e. if the concentration and the temperature are suddenly altered to T_1 and C_1 at the boundary, and maintained constant, the actual concentration and temperature can be calculated by Eq. 4:

$$\Delta T(t,x) = \Delta_0 T \phi_2(t,x) - \frac{\left(1-\mu_2^2\alpha'\right)\Delta_0 T - v\Delta_0 C}{\alpha'\left(\mu_1^2-\mu_2^2\right)}\left[\phi_2(t,x)-\phi_1(t,x)\right] \tag{4a}$$

$$\Delta C(t,x) = \Delta_0 C \phi_1(t,x) - \frac{\left(1-\mu_1^2 D'\right)\Delta_0 C - \lambda\Delta_0 T}{D'\left(\mu_1^2-\mu_2^2\right)}\left[\phi_2(t,x)-\phi_1(t,x)\right] \tag{4b}$$

where $\Delta T = T - T_0$, $\Delta C = C - C_0$, $\Delta_0 T = T_1 - T_0$, $\Delta_0 C = C_1 - C_0$, $\alpha' = \alpha/(1+\Delta H\omega/C_P)$, $v = \Delta H\sigma/C_P/(1+\Delta H\omega/C_P)$, $D' = D/[1 + (1-v)\rho_s\sigma/v]$, $\lambda = [(1-v)\rho_s\omega/v]/[1 + (1-v)\rho_s\sigma/v]$. The μ_i are the two roots of the equation :

$$(D'\mu^2 - 1)(\alpha'\mu^2 - 1) = \lambda v \tag{5}$$

The $\phi_i(t, x)$ are the solutions of ordinary diffusion equations with coefficients $D_i = 1/\mu_i$. For a slab of thickness $2b$ they read [4, p. 47]:

$$\phi_i(t,x) = 1 - \frac{4}{\pi}\sum_{n=0}^{\infty}\frac{(-1)^n}{2n+1}\exp\left[-\frac{(2n+1)^2\pi^2}{4}\frac{D_i t}{b^2}\right] \times \cos\left[\frac{(2n+1)\pi}{2}\frac{x}{b}\right] \tag{6}$$

Giving to the physical parameters appropriated values, the results of the analytical solution for Eq. 4a are reported as curves in Fig. 1, for 60, 300, 1,800, 7,200 and 14,400 s after the sudden change in external conditions (temperature raise $\Delta_0 T$ of 20 °C, and moisture increase $\Delta_0 C$ of 1 kg m^{-3}).

The generalized code can simulate the situation depicted above simply setting the code parameters as described in Table 2. Further assumption is the rectangular geometry (the flag has to be $f = 0$). The simulation has been performed by setting $\Delta t = 0.01$ s (time step), and $\Delta\xi = 0.005$ m (spatial step). Being the total time equal to 14,400 s, the resulting grid was $1{,}440{,}000 \times 20 = 28{,}800{,}000$ points. Predictions of numerical code are reported in Fig. 1 (temperature profile evolution in the textile package) as symbols. The numerical solution is in good agreement with the analytical one: by this way, the numerical code can be considered as validated.

4 A real process: DSC heating of foodstuff

4.1 Introduction

Detailed temperature and moisture profiles knowledge inside food samples during heating treatments (cooking,

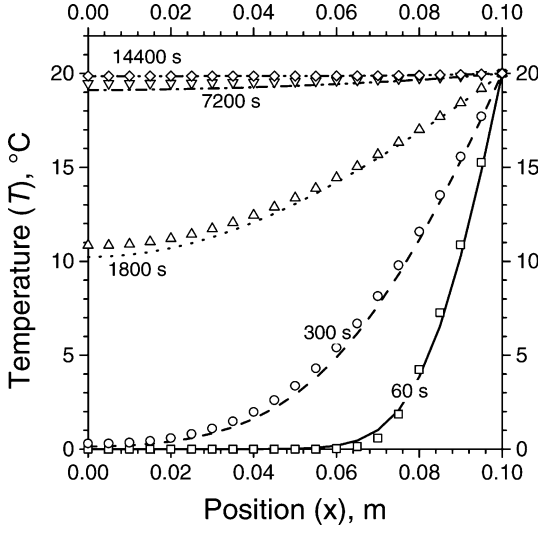

Fig. 1 Temperature profile evolution in a textile package (slab 0.2 m thickness), subject to a sudden change of external conditions ($\Delta_0 T = 20$ °C, see text). Analytical (*curves*) versus numerical solution (*symbols*)

Table 2 Values of code parameters to simulate the process described in Sect. 3 (a preliminary validation: the non-isothermal uptake of water by a textile package)

$\alpha_{A,1}$	$\beta_{A,1}$	$\gamma_{A,1}$	$\alpha_{B,1}$	$\beta_{B,1}$	$\gamma_{B,1}$	A_1	B_1
1	0	0	0	1	$-\Delta_0 T$	α'	$v\partial C/\partial t$
$\alpha_{A,2}$	$\beta_{A,2}$	$\gamma_{A,2}$	$\alpha_{B,2}$	$\beta_{B,2}$	$\gamma_{B,2}$	A_2	B_2
1	0	0	0	1	$-\Delta_0 C$	D'	$\lambda\partial T/\partial t$

drying, thawing) is highly desirable. Design and management of food treatment processes can be strongly improved by this knowledge, as obtained by the complete modeling of all the heat and mass transfer phenomena taking place in the samples.

The code developed in the frame of this work has been applied to the heating of a water-rich material foodstuff, accounting for all the most important transport phenomena. Experimental and modeling details, as well as related results, are reported below.

4.2 Experimental

Experimental runs were carried out in a Mettler DSC30 using slabs of raw potato (*Solanum tuberosum*, Agria *cultivar*) as model food. Potatoes are representative of a large range of high moisture food and have several features (such as small and homogeneous cells and structurally are less complex than other vegetables) useful to describe their characteristics by simplified relationships.

The samples were thin slabs of different thickness b (Fig. 2). The DSC pans were sealed and a hole was made in the cover, to allow the vapor elimination. For each sample, weight and thickness were recorded before and after the heat treatment. The initial moisture (kg water/kg drysolid) was calculated by

$$M_0 = \frac{\text{initial weight} - \text{final weight}}{\text{final weight}} \tag{7}$$

4.3 Modeling

For the DSC heating of a thin slab, the transient one-dimensional balance equations could be written as follows

$$\frac{\partial T}{\partial t} = \frac{k_{\mathrm{T},p}}{\rho_p C_{\mathrm{P},p}} \frac{\partial^2 T}{\partial \xi^2} \tag{8a}$$

$$\frac{\partial M}{\partial t} = D_{\mathrm{wp}} \frac{\partial^2 M}{\partial \xi^2} \tag{8b}$$

with the following initial conditions (initial temperature T_0 and initial moisture M_0):

$$\text{I.C.} \quad T(t=0,\xi) = T_0 \tag{9a}$$

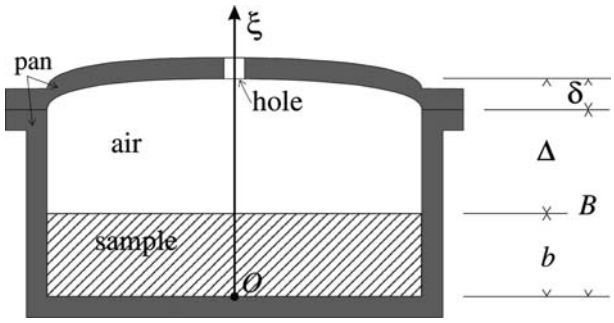

Fig. 2 DSC pan schematic

$$M(t=0,\xi) = M_0 \tag{9b}$$

Equation 8b assumes the water transport in liquid phase through the material [11].

The boundary condition on the bottom of the pan sets the sample temperature equal to the furnace temperature $T_{\mathrm{f}}(t)$ and the moisture flux as nil:

$$\text{B.C. } 1, @\xi = 0 \quad T(t,\xi=0) = T_{\mathrm{f}}(t) \tag{10a}$$

$$\left.\frac{\partial M}{\partial \xi}\right|_{\xi=0} = 0 \tag{10b}$$

Finally, the heat boundary condition (Eq. 11a) over the sample surface ($\xi = b$, inside the sealed pan) sets the conductive heat flow equal to the convection from the hot air to the sample plus the latent heat removed with water evaporation. In the same position the pseudo-diffusive moisture flow inside the sample was equated to the convection in the upper air.

$$\text{B.C. } 2, @\xi = b \quad -k_{\mathrm{T}} \left.\frac{\partial T}{\partial \xi}\right|_{\xi=b} = h\left(T|_{\xi=b} - T_f(t)\right) + \Delta H r_v'' \tag{11a}$$

$$-\rho D_{\mathrm{wp}} \left.\frac{\partial M}{\partial \xi}\right|_{\xi=b} = k_c\left(C_{\mathrm{surf}}\left(M|_{\xi=b}\right) - C_\infty\right) = r_v'' \tag{11b}$$

Material properties were found in literature and are summarized in Table 3. The system of PDEs (Eq. 8) plus initial (Eq. 9) and boundary conditions (Eqs. 10 and 11) has been solved by the generalized numerical code developed in this work, adopting the code parameters summarized in Table 4. The simulations have been performed by setting $\Delta t = 1$ s (time step) and dividing the slab thickness in 20 spatial steps (the spatial step value depends upon the slab thickness).

However, implementation of boundary condition 2 deserves further considerations:

1. The heat transfer phenomena from the upper surface of the sample consist of a term accounting for convection and radiation, plus a term accounting for latent heat depletion due to water evaporation. For the particular situation under observation, to our

Table 3 Material parameters to simulate the process described in Sec. 4 (a real process: the heating of foodstuff in a DSC)

Parameter (units)	Formula	Source
Water concentration in air on potato surface (kg m^{-3})	$C_{surf}(T,M) = f_s(T)g(M)$ $f_s(T) = \frac{(2.166\cdot 10^{-3})}{T} P_w^{sat}(T)$ $g(M) = \left(\frac{M}{0.0813}\right)^{1/0.458}\left[1+\left(\frac{M}{0.0813}\right)^{1/0.458}\right]^{-1}$	This work, elaboration from Refs. [11–13]
Conductivity of potato (W m^{-1} K^{-1})	$k_{T,p}(T,M) = \begin{cases} 0.1 & \text{if } M \leqslant 0.25 \\ 0.276 + 0.293\log(M) & \text{if } M > 0.25 \end{cases}$	This work Ref. [14]
Specific heat of potato (J kg^{-1} K^{-1})	$C_{P,p}(T,M) = (30.125) + (6.109)T + (849.4)M + (-104.2)M^2$	This work, elaboration from Ref. [15]
Diffusivity of water in potato (m^2 s^{-1})	$D_{wp}(T) = \left(3.446\cdot 10^{-7}\right)\cdot\exp\left(-\frac{2514}{T}\right)$	[16]
Density of potato (kg m^{-3})	$\rho_p(T,M) = 1079 + \exp\left(-0.383\cdot M^2\right) \times\left[190 + \frac{320-190}{1+\exp\left(\frac{T-318.9}{3.53}\right)}\right]$	This work, elaboration from (Wang and Brennan, 1995) data.
Saturation pressure of water in air (Pa)	$P_w^{sat}(T) = \exp\left(23.1699 - \frac{3799.89}{T-46.8}\right)$	These formulas are tuned on the basis of data reported by (Perry and Green [17]) (T in K)
Latent heat of evaporation of water (J kg^{-1})	$\Delta H_w(T) = \left(-2.43\cdot 10^3\right)\cdot T + \left(3.16\cdot 10^6\right)$	
Conductivity of air (W m^{-1} K^{-1})	$k_{Ta}(T) = \left(-2.56\cdot 10^{-8}\right)\cdot T^2 + +\left(9.27\cdot 10^{-5}\right)\cdot T + \left(5.29\cdot 10^{-4}\right)$	
Diffusivity of water in air (m^2 s^{-1})	$D_{wa}(T) = \left(1.95\cdot 10^{-4}\right)\cdot\exp\left(-\frac{595.7}{T}\right)$	

knowledge, no faithful correlation exists to estimate the heat transfer coefficient h in Eq. 11a. Thus, it has firstly been evaluated the order of magnitude of the heat transfer coefficient by the film theory, for which $h \approx k_{Ta}/\Delta$ (k_{Ta} and Δ being the air thermal conductivity and the thickness of the free space between the upper surface of the sample and the cover of the DSC pan, respectively, see Fig. 2). Finally, it has been selected the value of h as the product $\kappa_1 \cdot k_{Ta}/\Delta$, i.e. the parameter κ_1 acts as an adjustable one (due to local air mixing and to radiation, κ_1 is expected to be larger than one).

2. The right-hand side of Eq. 11b accounts for apparent density of dry solids, i.e. the amount of dry solids in 1 m^3 of sample volume: $\rho = \rho_p/(1 + M)$, since ρ = kg dry solids per m^3, ρ_p = kg potato per m^{-3}, M = kg water per kg dry solid.
3. A reasoning similar to the one of point (1) can be carried out for water vapor development from upper surface (B.C. 2, Eq. 11b). The order of magnitude of the mass transfer coefficient (k_c) could be estimated as $k_c = D_{wa}/\Delta$ (D_{wa} being the diffusivity of water vapor in air), the concentration of water in air close to the surface of the sample, C_{surf}, can be estimated by the equation in the first row of Table 3. However, no tested method exists for the water vapor concentration in the pan free space, C_∞, even if a value of the same order of magnitude of C_{surf} is expected, since the removal of water from the pan should be a slow phenomenon. To overcome these problems, the left-hand side of Eq. 11b has been rewritten as $(D_{wa}/\Delta)(C_{surf} - \kappa_2 \cdot C_{surf}) = (D_{wa}/\Delta)\cdot C_{surf}\cdot(1-\kappa_2)$, being κ_2 another adjustable parameter expected to be close to 1.
4. Even if the left-hand side of Eq. 11b built in point iii. could be directly implemented in the code, to avoid numerical instability (and to minimize the required number of time steps), the dependence of C_{surf} from moisture M, expressed by the function $g(M)$ in Table 3, has been linearized as a Taylor series: $g(M) = g(M^*) + g'(M^*)(M - M^*)$. Therefore, the left-hand side of Eq. 11b thus become: $(D_{wa}/\Delta)(1-\kappa_2)f_s(T)[g(M^*) + g'(M^*)(M - M^*)]$. Hence, the code parameters useful to reproduce boundary condition 2 for mass transfer will be: $\alpha_{A,2} = \rho D_{wp}$, $\beta_{A,2} = (D_{wa}/\Delta)(1-\kappa_2)f_s(T)g'(M^*)$, and $\gamma_{A,2} = (D_{wa}/\Delta)(1-\kappa_2)f_s(T)[g(M^*) - g'(M^*)\ M^*]$, M^* being the moisture close to the sample surface.

Finally, the heat flow as recorded by the DSC apparatus has been simulated [6] as

$$\phi(t) = -\frac{Sk_T}{m_s}\frac{\partial T}{\partial \xi}\bigg|_{\xi=b} = -\frac{k_T}{\rho_p b}\frac{\partial T}{\partial \xi}\bigg|_{\xi=b} \tag{12}$$

where S is the heat exchange surface and m_s is the sample mass.

Table 4 Values of code parameters to simulate the process described in Sec. 4 (a real process: the heating of foodstuff in a DSC)

$\alpha_{A,1}$	$\beta_{A,1}$	$\gamma_{A,1}$	$\alpha_{B,1}$	$\beta_{B,1}$	$\gamma_{B,1}$	A_1	B_1
0	1	$-T_f(t)$	k_T	h	$-hT_f + \Delta H r_v''$	$\alpha_{T,p}$	0
$\alpha_{A,2}$	$\beta_{A,2}$	$\gamma_{A,2}$	$\alpha_{B,2}$	$\beta_{B,2}$	$\gamma_{B,2}$	A_2	B_2
1	0	0	See text	See text	See text	D_{wp}	0

4.4 Results and discussion

The heating of a 400 μm thickness slab of potato, with an initial moisture content $M_0 = 4$ kg water per kg dry solids, starting from 25 °C until 250 °C in a DSC with a heating rate of 10 °C per min^{-1} has been experimentally carried out and, then, simulated ($b = 400$ μm; $\Delta = B$ +

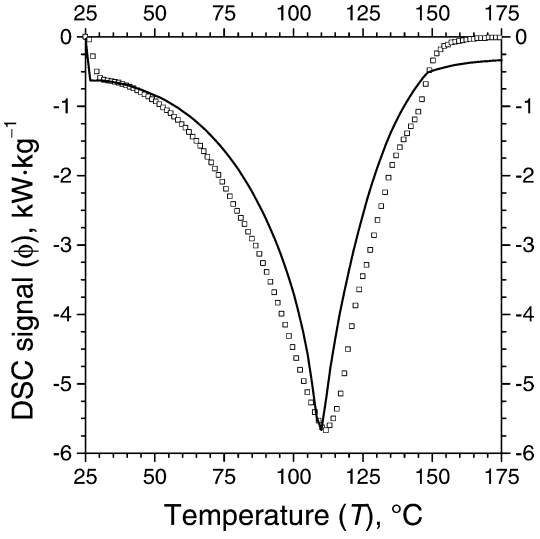

Fig. 3 DSC heating of a thin potato slab: experimental (*symbols*) and simulated (*solid line*) DSC signal

$\delta - b = 1700$ μm, see Fig. 2; $\kappa_1 = 42$, $\kappa_2 = 0.93$). The experimental DSC signal, as recorded during the heating run, is reported in Figure 3 (symbols). The simulated DSC signal, as calculated by eq. 12, is reported in Fig. 3 (solid line). The model is able to capture all the main features of the experimental signal, even if it does not perfectly reproduce the data. It is worth noticing that the material parameters have been taken from literature, sometimes forcing their original physical range of applicability (related measurements have been carried out in limited thermal range [11–15]. However, the validation has to be considered largely successful, since the position and the amplitude of the DSC peak is perfectly predicted.

Once the temperature and the moisture predicted by the code were validated, it is possible to gain insight the evolution of internal profiles. Thus, Fig. 4 reports temperature and moisture profiles at different times during the heating. The thermal distribution results to be essentially isothermal, whereas pronounced moisture gradients develop during the heating. These are key information for food processing management (for example, large residual humidity, in any position through the food can cause deterioration during a subsequent storing).

5 Conclusions

Starting from the generalization of the heat balance equation, in transient condition and along one-dimension, already presented in Barba and Lamberti [5], in this work a code able to numerically solve a couple of generalized balance equations (e.g. heat and mass transfer) is developed. The code was validated by comparison with the analytical solution known for a problem involving simultaneous heat and mass transfer, and was

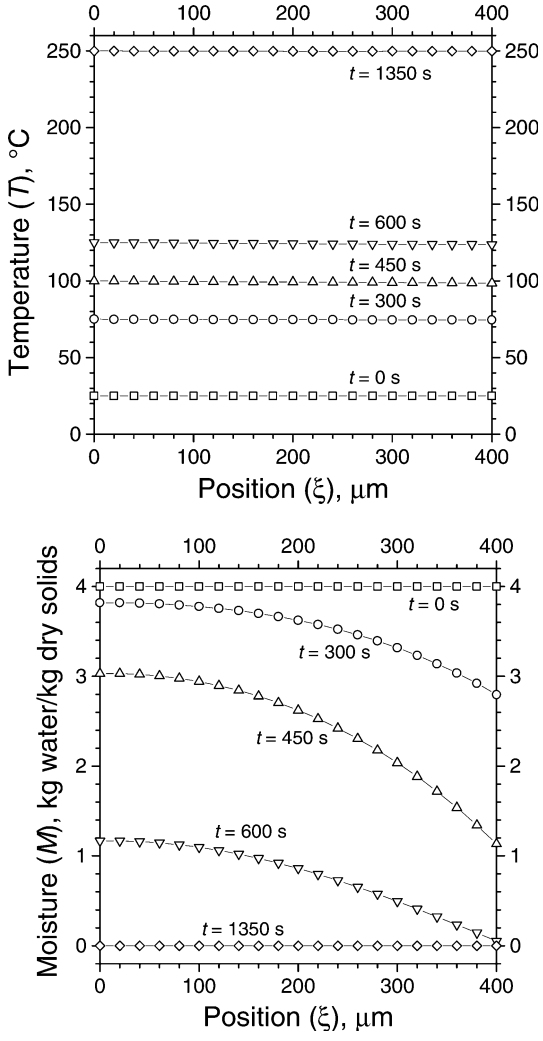

Fig. 4 DSC heating of a thin potato slab: (*above*) simulated temperature profiles (*below*) simulated moisture profiles

applied to describe the heating of foodstuff in a DSC pan. The code results well agree with the experimental DSC signal, confirming the model to be predictive.

The code can manage: (1) almost all the kind of boundary conditions; (2) variable coefficients; (3) multilayers problems; (4) different kinds of generation terms. It then constitutes a powerful tool for industrial and R&D studies. Attention will be dedicated, in future works, to the simulation of more complex food heating treatments performed by microwave energy: drying, cooking and thawing of foodstuffs.

Acknowledgements This study was supported by the Centro Regionale di Competenza sulle Produzioni Agro-Alimentari, P.O.R. 2000–2006.

References

1. Nijhuis HN, Torringa HM, Muresan S, Yuksel D, Leguijt C, Kloek W (1998) Approaches to improving the quality of dried fruit and vegetables. Trends Food Sci Technol 9:13–20

2. Bird RB, Stewart WE, Lightfoot EN (1960) Transport phenomena. Wiley, New York
3. Carslaw HS, Jaeger JC (1959) Conduction of heat in solids. Oxford University Press, London
4. Crank J (1975) The mathematics of diffusion. Oxford University Press, London
5. Barba AA, Lamberti G (2003) Preliminary validation of a numerical code for heat transfer simulations. Heat Mass Transfer 39(5–6):429–433
6. Lamberti G (2004) Importance of heat transfer phenomena during polymer solidification. Heat Mass Transfer 41(1):23–31
7. Acierno D, Barba AA, d'Amore M (2004) Heat transfer phenomena during processing materials with microwave energy. Heat Mass Transfer 40(5):413–420
8. Lapidus L, Pinder GF (1982) Numerical solution of partial differential equations in science and engineering. Wiley, New York
9. Henry PSH (1939) Diffusion in absorbing media. Proc R Soc 171A:215–241
10. Henry PSH (1948) The diffusion of moisture and heat through textiles. Discuss Faraday Soc 3:243–257
11. Wang N, Brennan JG (1995a) A mathematical model of simultaneous heat and moisture transfer during drying of potato. J Food Eng 24:47–60
12. Wang N, Brennan JG (1995b) Changes in structure, density and porosity of potato during dehydration. J Food Eng 24:61–76
13. Wang N, Brennan JG (1991) Moisture sorption isotherm characteristic of potatoes at four temperatures. J Food Eng 14:269–287
14. Wang N, Brennan JG (1992) Thermal conductivity of potato as a function of moisture content. J Food Eng 17:153–160
15. Wang N, Brennan JG (1993) The influence of moisture content and temperature on the specific heat of potato measured by differential scanning calorimetry. J Food Eng 19:303–310
16. Rovedo CO, Suarez C, Viollaz P (1998) Analysis of moisture profiles, mass biot number and driving forces during drying of potato slabs. J Food Eng 36:211–231
17. Perry RH, Green D (1984) Perry's chemical engineers' handbook. McGraw-Hill, New York